51st AIAA/ASME/ASCE/AHS/ASC Structures, Structural Dynamics, and Materials Conference
 18th
12 - 15 April 2010, Orlando, Florida

AIAA 2010-3118

Fluid-Structure Transient Gust Response Sensitivity for a Nonlinear Joined Wing Model

Shaobin Liu[1], Douglas P. Wickert[2], Robert A. Canfield[3]
Virginia Tech, Blacksburg, VA, 24061, USA

A continuous sensitivity analysis of the transient gust response for a one-dimensional joined wing model is developed. In continuous sensitivity methods, one computes design or shape parameter gradients from the continuous system of partial differential equations instead of the discretized system. The continuous sensitivity equations are a linear boundary-value problem which renders computationally efficient design parameter gradients without needing to derive and code the problematic mesh sensitivities of discrete sensitivity methods. The nonlinear fluid is modeled using quasi-steady compressible potential flow and the joined wing is modeled using nonlinear 1D beam elements. The coupled fluid-structure physics and continuous sensitivity system equations for a representative nonlinear gust response problem are posed and solved. Buckling sensitivity of the aft wing to several design and shape parameters is studied. Continuous sensitivity results for both the local and total material derivatives are presented and compared to gradients obtained by finite-difference methods.

I. Introduction

Ongoing research efforts are seeking new methods for effective and computationally efficient analysis to support large-scale design optimization of elastic aircraft structures. One aspect of these efforts are high-fidelity, nonlinear, aeroelastic models suitable for aircraft gust response [1, 2]. Of particular interest is the inverse design of a joined wing configuration (Figure 1) proposed for the next-generation of USAF persistent Intelligence, Surveillance, and Reconnaissance (ISR) aerospace platforms. A critical mission requirement is long endurance which dictates large fuel fractions and lightweight structures. The lightweight requirements and large aspect ratio of these configurations contribute to large deformations of the structure and significant geometrically nonlinear effects. Further, the low wing-loading results in significant gust response. Indeed gust response loads have been identified as the critical load condition for joined wing configurations similar to the designs of interest. Aeroelasticity is a challenging science, dealing with the interaction of two very different domains governed by disparate physics. Nonlinear aspects of both the fluid and structural domains can make accurate calculations of the interaction problematic, not the least due to the substantial computational expenses involved. Since optimization and inverse design methods typically require some measure of the change of an objective function or performance parameter to variations in design parameters, optimization of aeroelastic problems, which are themselves computationally intensive, challenging, and expensive to solve, can be outright formidable. Thus, this subject represents a prime frontier for basic research

In the continuous sensitivity method, also known as variational shape design [3], the continuum sensitivity method [5], and the variational sensitivity method [6], the design parameter gradients are calculated by solving the

The views expressed in this paper are those of the author and do not reflect the official policy or position of the United States Air Force, Department of Defense, or the United States Government.

[1] PhD Candidate, Department of Aerospace and Ocean Engineering, 214 Randolph Hall, Blacksburg VA, 24061.

[2] PhD Candidate, Department of Aeronautical and Astronautical Engineering, 2950 Hobson Way, Wright-Patterson AFB, OH 45433-7765, AIAA Member

[3] Professor, Department of Aerospace and Ocean Engineering, 214 Randolph Hall, Blacksburg VA, 24061, AIAA Associate Fellow.

continuous sensitivity equations (CSE), typically a system of partial differential equations [7]. Since the CSE system is posed as a continuous system, it can efficiently produce shape parameter gradients without calculating the mesh sensitivity (which often amounts to the expensive task of inverting a large mesh Jacobian). Further, the sensitivity system is always a linear system of equations, even when the original system is nonlinear.

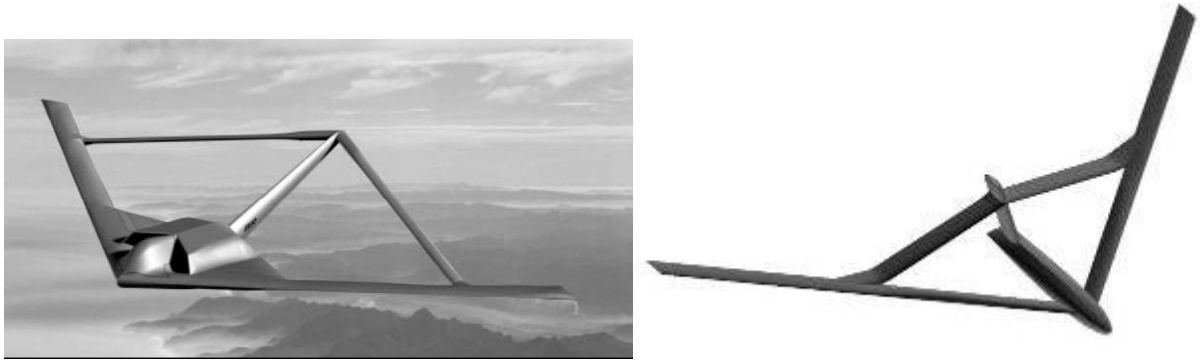

Figure 1: Boeing design study (left) and AFRL Sensor-Craft concept (right) joined wing configurations

Continuous sensitivity methods were first introduced for structural problems [5, 8], but few applications to structural problems appear in the literature. The landmark Borggaard and Burns paper [9] introduced the CSE nomenclature in a fluid setting and several fluid flow optimization applications followed [7, 10-12]. Although there now exists an extensive body of literature describing and documenting the application of continuous sensitivity methods to fluid dynamics problems, the applications to non-fluid problems have largely been limited to 1-D scalar problems (*e.g.* heat flow) and 1-D beam problems [12]. Bhaskaran and Berkooz [10] present an FEM-based continuous sensitivity solution for a 2-D structural elasticity problem that is also considered in [13], but there remains a dearth of structural elasticity applications that employ continuous sensitivity methods. Pelletier *et al.* have employed continuous sensitivity methods for a range of fluid-structure interaction problems [14-16] with prominent success, however much of their work focuses on flow variable sensitivities. Recent work [2] has applied the CSE method to the gust sensitivity for simple airfoils mounted to a 1D structure. The current effort extends this method to a nonlinear joined wing.

Continuous sensitivity systems are typically posed in terms of local derivatives (an Eulerian reference frame), though it is possible to derive the CSE system in total derivative form (Lagrangian reference frame [17]). For shape optimization of fluid applications, an Eulerian description of the flow sensitivity is usually adequate. Thus, much of the literature does not emphasize the distinction between the local and total derivative. For structural optimization problems, however, the design sensitivity at a material point is usually required, which necessitates a means to convert the local sensitivities from the CSE solution to total sensitivities at a given material point. We describe this conversion and present a simple example that illustrates the distinction between the local and total derivatives.

This paper begins with a derivation of the continuous sensitivity system and its associated boundary conditions. The next section describes a fluid-structure problem that is fairly simple to describe and solve yet complex enough to capture all the salient aspects of a continuous sensitivity calculation for a coupled domain, nonlinear, transient system. This is followed by a brief description of the computational approach used to solve both the transient, nonlinear fluid-structure system and the CSE system. The form of the linear CSE system is described and contrasted with the form of the nonlinear fluid-structure system. The sensitivity conversion between the local and total derivatives is demonstrated and shape parameter gradients are used to extrapolate the transient response to a design variation of the problem. The results are compared with both finite difference calculations and numerical solutions of the perturbed system.

II. Continuous Sensitivity Equations

Consider the following general, nonlinear boundary value system defined in a domain Ω with a boundary Γ for which we seek a solution **u** of the equations

$$\mathbf{A}(\mathbf{u})\mathbf{u} = \mathbf{f} \text{ in } \Omega \tag{1}$$

$$\mathbf{B}(\mathbf{u})\mathbf{u} = \mathbf{g} \text{ on } \Gamma \tag{2}$$

where $\mathbf{A}(\mathbf{u})$ is a first-order, time-space differential operator given by

$$\mathbf{A} = \mathbf{A}_t \frac{\partial}{\partial t} + \sum_{i=1}^{\dim} \mathbf{A}_i \frac{\partial}{\partial x_i} + \mathbf{A}_0 \tag{3}$$

The system is nonlinear if the operator **A** is a function of the solution **u**, or $\mathbf{B}(\mathbf{u})$,the boundary operator

$$\mathbf{B} = \mathbf{B}_t \frac{\partial}{\partial t} + \sum_{i=1}^{\dim-1} \mathbf{B}_i \frac{\partial}{\partial \xi_i} + \mathbf{B}_0 \tag{4}$$

is a function of **u**. The boundary operator (4) specifies the boundary condition (solution) for **u** on Γ. In (4), ξ_i denotes the coordinates that parameterize the boundary which are naturally at least one dimension less than the domain dimension.

The sensitivity of the solution **u** to a design parameter, *b*, is $\frac{\partial \mathbf{u}}{\partial b}$. For example, the first forward difference for approximating the design sensitivity is

$$\frac{\partial \mathbf{u}}{\partial b} \approx \Delta_b(\mathbf{u}) = \frac{\mathbf{u}(b+\delta b) - \mathbf{u}(b)}{\delta b} \tag{5}$$

Besides the computational expense involved in solving the system twice, a drawback of the finite difference method is the challenge of determining the optimum step size, δb. Large steps are dominated by truncation error (which can be significant if the system is nonlinear) and small steps are dominated by numerical round-off error. Another shortcoming of the finite difference approach when *b* represents a shape parameter is that the finite difference calculation approximates the material (or total) derivative and not the desired local derivative, $\frac{\partial \mathbf{u}}{\partial b}$.

The continuous sensitivity method avoids the numerical shortcomings of finite difference methods by differentiating the field equations (3.1-3.2) to yield a governing continuous system of equations for the desired sensitivity variables. So differentiating (1) with respect to a design parameter, *b*, yields

$$\frac{\partial}{\partial b}\left[\mathbf{A}_0(\mathbf{u};b)\mathbf{u} + \mathbf{A}_i(\mathbf{u};b)\mathbf{u}_{,i} + \mathbf{A}_t(\mathbf{u};b)\mathbf{u}_{,t}\right] = \frac{\partial}{\partial b}\left[\mathbf{f}(\mathbf{x};b)\right] \tag{6}$$

where the subscripted comma notation denotes partial differentiation. Equation (6) in component form (with Einstein summation notation implied) is

$$\frac{\partial}{\partial b}\left[a_{ij}^{(0)}(\mathbf{u};b)u_j + a_{ij}^{(k)}(\mathbf{u};b)u_{j,k} + a_{ij}^{(t)}(\mathbf{u};b)u_{j,t}\right] = \frac{\partial}{\partial b}\left[f_i(\mathbf{x};b)\right] \tag{7}$$

where the parenthetical superscript is used to denote the operator. Thus, *k* is an index ranging from one up to the domain dimension, n_{domain}. Equation (7) expands as

$$\left[\frac{\partial a_{ij}^{(0)}}{\partial b}u_j+\frac{\partial a_{ij}^{(0)}}{\partial u_m}\frac{\partial u_m}{\partial b}u_j+a_{ij}^{(0)}\frac{\partial u_j}{\partial b}\right]+\left[\frac{\partial a_{ij}^{(k)}}{\partial b}u_{j,k}+\frac{\partial a_{ij}^{(k)}}{\partial u_m}\frac{\partial u_m}{\partial b}u_{j,k}+a_{ij}^{(k)}\frac{\partial u_{j,k}}{\partial b}\right]+\ldots$$
$$\frac{\partial a_{ij}^{(t)}}{\partial b}u_{j,t}+\frac{\partial a_{ij}^{(t)}}{\partial u_m}\frac{\partial u_m}{\partial b}u_{j,t}+a_{ij}^{(t)}\frac{\partial u_{j,t}}{\partial b}=\frac{\partial}{\partial b}f_i\left(\mathbf{x};b\right) \tag{8}$$

Since the spatial-temporal derivatives are independent operations from the sensitivity derivative, the order of differentiation may be reversed. Note that this commutation of differentiation is not possible if the sensitivity derivative in (6) is not a local derivative [59]. The $\frac{\partial u_m}{\partial b}$ terms are referred to as the sensitivity variables; they represent how the solution changes with respect to a design parameter. Collecting the sensitivity variables in (8) then yields the continuous sensitivity system

$$\left[a_{im}^{(0)}+\frac{\partial a_{ij}^{(0)}}{\partial u_m}u_j+\frac{\partial a_{ij}^{(k)}}{\partial u_m}u_{j,k}+\frac{\partial a_{ij}^{(t)}}{\partial u_m}u_{j,t}\right]\frac{\partial u_m}{b}+\left[a_{im}^{(k)}\right]\frac{\partial u_{m,k}}{\partial b}+\left[a_{im}^{(t)}\right]\frac{\partial u_{m,t}}{\partial b}=$$
$$\frac{\partial}{\partial b}f_i\left(\mathbf{x};b\right)-\left[u_j\frac{\partial a_{ij}^{(0)}}{\partial b}+u_{j,k}\frac{\partial a_{ij}^{(k)}}{\partial b}+u_{j,t}\frac{\partial a_{ij}^{(t)}}{\partial b}\right] \tag{9}$$

Notice that (9) is in the same form as (1) with (3) operating on the sensitivity variable $\mathbf{u}_{,b}$ instead of the original field variable $\mathbf{u}$. That is

$$\left[{}^{b}\mathbf{A}_0\right]\mathbf{u}_{,b}+\left[\mathbf{A}_i\right]\left(\mathbf{u}_{,b}\right)_{,i}+\left[\mathbf{A}_t\right]\left(\mathbf{u}_{,b}\right)_{,t}=\mathbf{f}_{,b}\left(\mathbf{x};b\right)-\left[\mathbf{A}_{0,b}\mathbf{u}+\mathbf{A}_{i,b}\mathbf{u}_{,i}+\mathbf{A}_{t,b}\mathbf{u}_{,t}\right] \tag{10}$$

The first bracketed matrix term in (10) is identified as the ${}^{b}\mathbf{A}_0$ sensitivity matrix, which is defined in component form by

$${}^{b}a_{ij}^{(0)}=a_{ij}^{(0)}+\frac{\partial a_{il}^{(0)}}{\partial u_j}u_l+\frac{\partial a_{il}^{(k)}}{\partial u_j}u_{l,k}+\frac{\partial a_{il}^{(t)}}{\partial u_j}u_{l,t} \tag{11}$$

This may also be expressed in matrix form as

$$\begin{aligned}{}^{b}\mathbf{A}_0=\mathbf{A}_0&+\mathbf{A}_{0,u_1}\left[\{\mathbf{u}\}\{0\}\ldots\{0\}\right]+\mathbf{A}_{0,u_2}\left[\{0\}\{\mathbf{u}\}\ldots\{0\}\right]+\mathbf{A}_{0,u_n}\left[\{0\}\ldots\{0\}\{\mathbf{u}\}\right]+\ldots\\&+\mathbf{A}_{1,u_1}\left[\left\{\mathbf{u}_{,x_1}\right\}\{0\}\ldots\{0\}\right]+\mathbf{A}_{1,u_2}\left[\{0\}\left\{\mathbf{u}_{,x_1}\right\}\ldots\{0\}\right]+\mathbf{A}_{1,u_n}\left[\{0\}\ldots\{0\}\left\{\mathbf{u}_{,x_1}\right\}\right]+\ldots\\&+\mathbf{A}_{n,u_1}\left[\left\{\mathbf{u}_{,x_n}\right\}\{0\}\ldots\{0\}\right]+\mathbf{A}_{n,u_2}\left[\{0\}\left\{\mathbf{u}_{,x_n}\right\}\ldots\{0\}\right]+\mathbf{A}_{n,u_n}\left[\{0\}\ldots\{0\}\left\{\mathbf{u}_{,x_n}\right\}\right]+\ldots\\&+\mathbf{A}_{t,u_1}\left[\left\{\mathbf{u}_{,t}\right\}\{0\}\ldots\{0\}\right]+\mathbf{A}_{t,u_2}\left[\{0\}\left\{\mathbf{u}_{,t}\right\}\ldots\{0\}\right]+\mathbf{A}_{t,u_n}\left[\{0\}\ldots\{0\}\left\{\mathbf{u}_{,t}\right\}\right]\end{aligned} \tag{12}$$

This may be written more compactly as

$${}^{b}\mathbf{A}_0=\mathbf{A}_0+\frac{\partial\mathbf{A}_0}{\partial u_i}\left[u_i\delta_{ji}\right]+\frac{\partial\mathbf{A}_k}{\partial u_i}\left[u_{i,k}\delta_{ji}\right]+\frac{\partial\mathbf{A}_t}{\partial u_i}\left[u_{i,t}\delta_{ji}\right] \tag{13}$$

Finally, the CSE system associated with (1) may be written in compact form as

$$\left(\frac{\partial \mathbf{A}}{\partial \mathbf{u}}\mathbf{u}_{\delta}+\mathbf{A}\right)^{b}\mathbf{u}={}^{b}\mathbf{f}-\frac{\partial \mathbf{A}}{\partial b}\mathbf{u} \tag{14}$$

where $\dfrac{\partial \mathbf{A}}{\partial \mathbf{u}}\mathbf{u}_{\delta}\equiv\dfrac{\partial \mathbf{A}}{\partial u_i}\left[u_i\delta_{ji}\right]$.

In (14) we introduce a superscript prefix notation, ${}^{b}\mathbf{u}$, to denote the sensitivity variable that is determined by solving the CSEs. In the examples below when an analytic solution is available, the ${}^{b}\mathbf{u}$ solution will be treated as distinct from an analytic sensitivity, denoted by $\mathbf{u}_{,b}$. The analytic solution notation will be used to represent the sensitivity determined by taking the derivative of an analytic solution $\mathbf{u}$ to equations (3.1-3.2). We also introduce notation for the finite difference operator, $\Delta_b(\mathbf{u})$, given by (5), and the material derivative operator, $D_b(\mathbf{u})$, defined in the next section.

Note that the gradient operators, the $\mathbf{A}_i$'s in (3), are unchanged for the CSE system, (10). Further, for linear systems, the sensitivity matrix ${}^{b}\mathbf{A}_0=\mathbf{A}_0$. Equation (9) includes both the explicit dependence of the system solution on *b* (*e.g.* as with sizing or shape sensitivity), as well as the implicit, nonlinear dependence of the system solution on *b* (*e.g.* as in shape optimization). Additionally, in shape sensitivity problems, where *b* represents a boundary shape parameter, the system operators typically have no explicit dependence on *b* and the brackets terms on the right-hand side of (10), *e.g.* $\mathbf{A}_{i,b}$, vanish. Thus, for linear, shape variation problems, the component CSE operators are identical to the original system operators.

Note also that the continuous sensitivity system (10) is always linear in the sensitivity variable, $\mathbf{u}_{,b}$, even when the original system is nonlinear. The conclusion that only the ${}^{b}\mathbf{A}_0$ operator changes for a nonlinear system is due to the assumption that system (3.1-3.2) only being nonlinear in $\mathbf{u}$. If the nonlinearity appeared explicitly in a derivative of $\mathbf{u}$, $\mathbf{u}_{,x}$ for example, then

$$\left[\mathbf{A}\left(\mathbf{u}_{,x}\right)\right](\cdot)=\sum_{i=1}^{\dim}\mathbf{A_i}\left(\mathbf{u}_{,x}\right)\frac{\partial}{\partial x_i}+\mathbf{A_0}\left(\mathbf{u}_{,x}\right) \tag{15}$$

and only the ${}^{b}\mathbf{A}_1$ component operator of the CSE system would differ from the component operators of the original system. The general conclusion is that the CSE system will differ from the parent system in whichever operator component represents the nonlinearity. Note that when the parent system is written in first-order form, the nonlinear problem can always be factored so that the nonlinearities appear explicitly in $\mathbf{u}$. Table 1 summarizes the form of the CSE operators in terms of the original system operators from (1) for both linear and nonlinear systems, as well as shape variation problems (with no explicit dependence on the design parameter) and non-shape variation problems with explicit dependence on the design parameter.

Table 1: Summary of CSE operators in first-order form

Problem Type	${}^{b}\mathbf{A}_0$	${}^{b}\mathbf{A}_k \quad k=1,\ldots,n_{dom},t$	${}^{b}\mathbf{f}$
Linear, shape	$\mathbf{A}_0$	$\mathbf{A}_k$	0
Linear, explicit *b* (size, material)	$\mathbf{A}_0$	$\mathbf{A}_k$	$\mathbf{f}_{,b}(\mathbf{x};b)-\left[\mathbf{A}_{0,b}\mathbf{u}+\mathbf{A}_{k,b}\mathbf{u}_{,k}\right]$
Nonlinear, shape	${}^{b}\mathbf{A}_0$	$\mathbf{A}_k$	0
Nonlinear, explicit *b* (size, material)	${}^{b}\mathbf{A}_0$	$\mathbf{A}_k$	$\mathbf{f}_{,b}(\mathbf{x};b)-\left[\mathbf{A}_{0,b}\mathbf{u}+\mathbf{A}_{k,b}\mathbf{u}_{,k}\right]$

The boundary conditions of the sensitivity equation specify how the sensitivity variables behave on the boundary of the domain. Thus, the sensitivity of the boundary operator system may be written as a first-order CSE system analogous to (14)

$$\left[\mathbf{B}_0+\frac{\partial\mathbf{B}_0}{\partial u_i}\left[\{u_i\}\delta_{ji}\right]+\frac{\partial\mathbf{B}_\xi}{\partial u_i}\left[\{u_{i,\xi}\}\delta_{ji}\right]\right]{}^{b}\mathbf{u}+\mathbf{B}_\xi\,{}^{b}\mathbf{u}_{,\xi}= \mathbf{g}_{,b}(\mathbf{x};b)-\left[\mathbf{B}_{0,b}\mathbf{u}+\mathbf{B}_{\xi,b}\mathbf{u}_{,\xi}\right] \quad \text{on } \Gamma(b) \tag{16}$$

where ξ denotes coordinates that parameterize the boundary (which has dimension of at least one less than the domain). The continuous sensitivity domain equations, (9), is simply another system of differential equations, which, given with the appropriate boundary data, (16), represents a well-posed boundary value problem that may be solved by a wide variety of numerical approaches. It is convenient in many cases to use the same numerical method and framework to solve the sensitivity system as was used to solve the original system.

For shape variation problems, the boundary Γ is a function of the design parameter *b* and the evaluation of (16) must account for the total variation of a material point on the boundary. For a scalar, *u*, the Eulerian and material points are related through the total (material) derivative

$$D_b(u)\equiv\left.\frac{Du}{Db}\right|_{\mathbf{X}}=\left.\frac{\partial u}{\partial b}\right|_{\mathbf{x}}+\nabla u\cdot\left.\frac{\partial\mathbf{X}_\Omega}{\partial b}\right|_{\mathbf{X}} \tag{17}$$

where $D_b(\cdot)$ is the material derivative operator with respect to the parameter *b*, **X** denotes a material coordinate and **x** denotes a spatial coordinate (Eulerian description). Thus the total derivative of *u* with respect to *b* at a material point **X** consists of the local derivative of *u* with respect to parameter *b* and the convective transport term which accounts for how the material point **X** moves as the design parameter *b* varies. For the vector quantity **u**, the local derivative, gradient operation, and dot product in (17) are carried out component-wise. Solving (17) for the local derivative gives the desired sensitivity boundary condition for the CSE system

$${}^{b}\mathbf{u}\big|_{\Gamma}\equiv\left.\frac{\partial\mathbf{u}}{\partial b}\right|_{\mathbf{X}=\Gamma}=\left.\frac{D\mathbf{u}}{Db}\right|_{\Gamma}-\nabla\mathbf{u}\cdot\frac{\partial\mathbf{X}_{\Gamma(b)}}{\partial b} \tag{18}$$

where in 2D

$$\mathbf{X}_{\Gamma(b)}=\left\{(x,y)\in\Gamma(b)\right\} \tag{19}$$

are the coordinates (ordered pairs in $\mathbf{R}^2$) that define the boundary as a function of *b*. The first term on the right side of (18) accounts for how the boundary conditions for the problem change with respect to the design parameter. This term is often zero; that is, the nature of the boundary condition often does not change as the shape changes. For example, the boundary conditions for the fixed end of a cantilevered beam are zero displacement and rotation at the root. A shape variation parameter can move the location of the root in an Eulerian reference frame, but the material point at the root will still be fixed and the displacement and rotation boundary conditions are still those of a cantilevered beam. Some examples are considered in Chapters 5 and 6 where the first term on the right-hand side of (18) does not vanish, but these tend to be the exception to most applications.

The transport term in (18) (the second term on the right-hand side) is the dot product of the derivative of the set of spatial coordinates that define the boundary with the gradient of the solution to (1)-(2). Again, in the case of vector quantities, the gradient operation is carried out row-wise.

To summarize, the continuous sensitivity system is a linear boundary value problem derived by taking the derivatives of the original field equations, (1-2). The set of sensitivity boundary condition data are of the same form as for the original problem; however, the boundary shape variation for shape sensitivity problems must be accounted for through (18). The continuous sensitivity equations may be derived in either total or local derivative form. When expressed in local form, only the boundary parameterization need be described. In total derivative form, the parameterization or transformation function for the entire domain is necessary which is equivalent to having to solve the mesh Jacobian. The domain Jacobian must also be solved and inverted for continuous sensitivity domain parameterization (total derivative) methods [6]. Posing the CSE in local derivative form and parameterizing the boundary as described above avoids the numerical complexity and expense of the mesh and domain Jacobian. Next we illustrate how to relate the local and total derivative sensitivity forms for a particular example.

III. Sting Mounted Typical Section Gust Model

Consider a flexible NACA 0012 airfoil mounted on a sting with a supporting strut. This simple two-dimensional model in Figure 2 has features representative of a three-dimensional joined wing. The three-beam model represents a two-dimensional analog to large spanwise deflection, chordwise deformation of the forward wing, and buckling of the aft wing. The sting and strut are modeled as nonlinear Euler-Bernoulli beams capable of large deflections. A beam to model chordwise bending is fixed to the chord line to represent the torsional deformation of a three-dimensional wing under aerodynamic load. At a positive angle of attack, the airfoil generates lift, deflecting the beam in the fluid, resulting in an increased angle of attack. Equilibrium deflection of the sting occurs when the force and moments generated by the lifting airfoil balance the internal sting force and moments resisting the bending. The strut is subject to a buckling load due to the deflection of the sting. Aerodynamic forces and moments on the airfoil are calculated using quasi-steady compressible flow aerodynamics. The airfoil coordinate system forces are

$$F_{x_a} = -\int_{LE}^{TE} p_u \cos\beta d\xi_u + \int_{LE}^{TE} p_l \cos\beta d\xi_l \tag{20}$$

$$F_{y_a} = \int_{LE}^{TE} p_u \sin\beta d\xi_u + \int_{LE}^{TE} p_l \sin\beta d\xi_l \tag{21}$$

The lift and drag are then

$$L = F_{y_a}\cos\alpha_{eff} - F_{x_a}\sin\alpha_{eff} \tag{22}$$

$$D = F_{x_a}\cos\alpha_{eff} + F_{y_a}\sin\alpha_{eff} \tag{23}$$

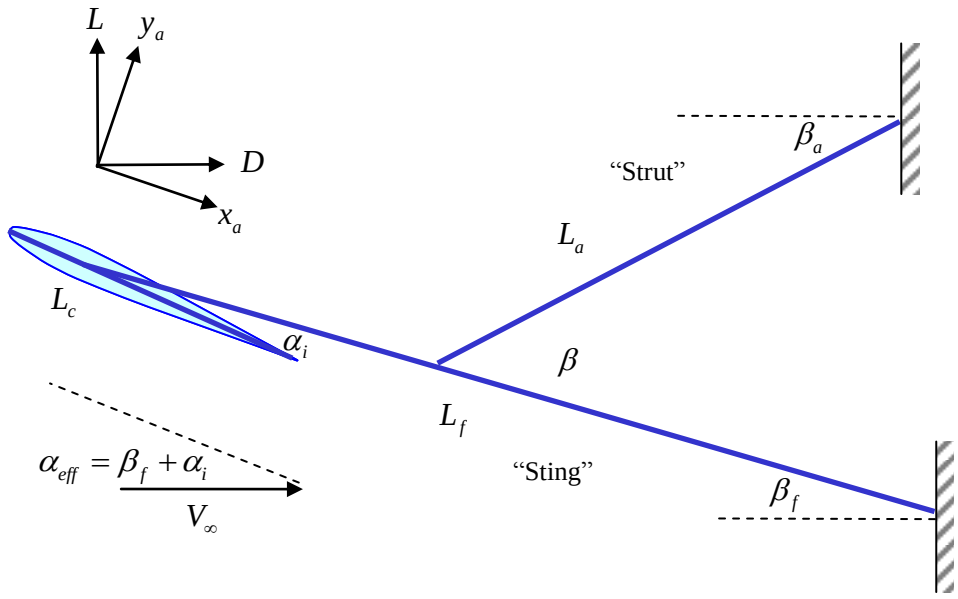

Figure 2: Joined Wing mounted airfoil

For shape sensitivity analysis, the length and angles of the forward and aft stings are taken as shape parameters

A. Gust Model

The vertical gust is modeled using the usual discrete gust idealization of a *one-minus-cosine* pulse [38], so that

$$V_g(t) = \begin{cases} \frac{1}{2} V_{g,\max} \left(1 - \cos \frac{2\pi (t - \tau_0)}{T_g} \right) & \tau_0 \le t \le T_g \\ 0 & o.w. \end{cases} \tag{24}$$

where $V_{g,\max}$ is the maximum amplitude of the gust, τ_0 is the start of the gust, and T_g is the duration of the gust. Since the NACA 0012 is symmetric and the tip of the sting is mounted at the aerodynamic center of the airfoil, the fluid moments are zero.

$$M_f = 0 \tag{25}$$

This model ignores unsteady aerodynamic effects and the time it takes for the gust to transit the chord of the airfoil, but it is sufficient for the current purpose.

The gust is not a function of beam length, so that

$$\frac{\partial}{\partial L} V_g(t) = 0 \tag{26}$$

B. Nonlinear Euler-Bernoulli Beam

The sting is modeled as a nonlinear Euler-Bernoulli beam where the nonlinear von Karman strain relations account for possible large deflections of the beam. We assume large transverse displacements, small strains, and moderate rotations. Since the changes in geometry are small, no distinction between the Piola-Kirchoff and Cauchy stress tensors is necessary [39].

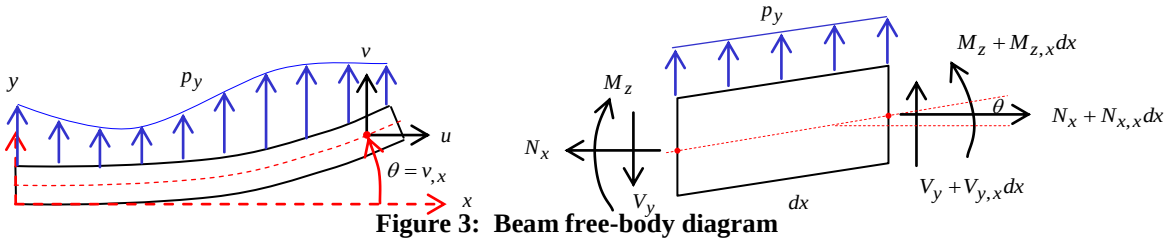

Figure 3: Beam free-body diagram

With the Euler-Bernoulli assumption, the angle of rotation and the internal bending moment are given by

$$\theta = v_{,x} \tag{27}$$

$$M_z = EI\theta_{,x} \tag{28}$$

where v is the vertical displacement, and the product of Young's modulus, E, and the moment of inertia, I, is the effective bending stiffness of the beam. The axial force, N_x, at any cross section of the beam is given by

$$N_x = \int_A \sigma_{xx} dA \tag{29}$$

where σ_{xx} is the normal stress and A is the cross sectional area of the beam. Summing the moments about the z-axis yields

$$M_{z,x} + V_y - N_x\theta = 0 \tag{30}$$

The nonlinear von Karman strain-displacement relation [106] in the axial direction is

$$\varepsilon_{xx} = u_{,x} + \tfrac{1}{2}\theta^2 \tag{31}$$

Spar buckling due to axial compression is a possible failure mode of joined wing configurations. Including an axial tip load, P_{tip}, then the von Karman strain together with the constitutive equation

$$\sigma_{xx} = E\varepsilon_{xx} \tag{32}$$

yields the nonlinear relationship between tip load, shear, bending moment, and rotation

$$M_{z,x} + V_y - P_{tip}\theta - \frac{EA}{2}\theta^3 = 0 \tag{33}$$

If there are no axial loads (so that the beam is inextensible beam and $u_{,x} = 0$), (33) reduces to

$$M_{z,x} + V_y - \frac{EA}{2}\theta^3 = 0 \tag{34}$$

Note that V_y is the shear force perpendicular to the x-axis, not the shear force, Q, perpendicular to the neutral axis of the deformed beam which is given by

$$Q = -V_y + \frac{EA}{2}\theta^3 \tag{35}$$

Finally, summing the forces in the y-direction yields the final equation governing the beam dynamics

$$\rho_y \frac{\partial^2 v}{\partial t^2} - V_{y,x} = p_y \tag{36}$$

where ρ_y is the mass per unit length of the sting and p_y is the transverse load per unit length. Substituting (34) and (28) into (36) yields the nonlinear governing equation large deflections, v, of the sting subject to a transverse load

$$\rho_y \frac{\partial^2 v}{\partial t^2} + \frac{\partial^2}{\partial x^2}\left(EI \frac{\partial^2 v}{\partial x^2} \right) - \frac{\partial}{\partial x}\left[\frac{EA}{2}\left(\frac{\partial v}{\partial x} \right)^3 \right] = p_y \tag{37}$$

The nonlinear beam system in first-order matrix operator form is

$$A_t \mathbf{u}_{,t} + A_0 \mathbf{u} + A_1 \mathbf{u}_{,x} = \mathbf{f} \tag{38}$$

where $\mathbf{u} = \begin{bmatrix} v & \theta & M_z & V_y & \dot{v} \end{bmatrix}^T$ and the matrix operators are

$$A_t = \begin{bmatrix} 0 & 0 & 0 & 0 & 0 \\ 0 & 0 & 0 & 0 & 0 \\ 0 & 0 & 0 & 0 & 0 \\ 0 & 0 & 0 & 0 & \rho_y \\ 1 & 0 & 0 & 0 & 0 \end{bmatrix} \quad A_0 = \begin{bmatrix} 0 & 1 & 0 & 0 & 0 \\ 0 & 0 & 1/EI & 0 & 0 \\ 0 & P_{tip} + \frac{1}{2} EA\theta^2 & 0 & -1 & 0 \\ 0 & 0 & 0 & 0 & 0 \\ 0 & 0 & 0 & 0 & -1 \end{bmatrix} \quad A_1 = \begin{bmatrix} -1 & 0 & 0 & 0 & 0 \\ 0 & -1 & 0 & 0 & 0 \\ 0 & 0 & -1 & 0 & 0 \\ 0 & 0 & 0 & 1 & 0 \\ 0 & 0 & 0 & 0 & 0 \end{bmatrix} \quad \mathbf{f} = \begin{bmatrix} 0 \\ 0 \\ 0 \\ p_y \\ 0 \end{bmatrix} \tag{39}$$

The system of continuous sensitivity equations is formed by differentiating (27), (28), (33), and (36). Thus the nonlinear beam CSEs in first order form are

$$^L\theta = {}^L v_{,x} \tag{40}$$

$$^L M_z = EI\, {}^L\theta_{,x} \tag{41}$$

$$^L M_{z,x} + {}^L V_y - P_{tip}\, {}^L\theta - \tfrac{3}{2} EA\theta^2 \left({}^L\theta \right) = 0 \tag{42}$$

$$\rho_y \left({}^L\dot{v} \right) - {}^L V_{y,x} = {}^L p_y \tag{43}$$

$$^L\dot{v} = {}^L v_{,t} \tag{44}$$

As noted above, the sensitivity system is linear, even though the original elasticity equations were nonlinear. In first-order, matrix operator form, (40)-(44) are

$${}^L A_t = \begin{bmatrix} 0 & 0 & 0 & 0 & 0 \\ 0 & 0 & 0 & 0 & 0 \\ 0 & 0 & 0 & 0 & 0 \\ 0 & 0 & 0 & 0 & \rho_y \\ 1 & 0 & 0 & 0 & 0 \end{bmatrix} \quad {}^L A_0 = \begin{bmatrix} 0 & 1 & 0 & 0 & 0 \\ 0 & 0 & 1/EI & 0 & 0 \\ 0 & P_{tip} + \frac{3}{2} EA\theta^2 & 0 & -1 & 0 \\ 0 & 0 & 0 & 0 & 0 \\ 0 & 0 & 0 & 0 & -1 \end{bmatrix} \quad {}^L A_1 = \begin{bmatrix} -1 & 0 & 0 & 0 & 0 \\ 0 & -1 & 0 & 0 & 0 \\ 0 & 0 & -1 & 0 & 0 \\ 0 & 0 & 0 & 1 & 0 \\ 0 & 0 & 0 & 0 & 0 \end{bmatrix} \quad {}^L\mathbf{f} = \begin{bmatrix} 0 \\ 0 \\ 0 \\ p_y \\ 0 \end{bmatrix} \tag{45}$$

Note that, as explained above, the A_t and A_1 CSE matrix operators are the same as the original, nonlinear elasticity system, but that the A_0 matrix for the CSE system is different.

The nonlinear bending strain term $-\frac{EA}{2}\theta^3$ is a stiffening term (the nonlinear bending strain absorbs some of the energy of the transverse load). If the axial tip force is tensile in nature ($P_{tip} > 0$) then the nonlinear effect is further stiffening. If the axial tip force is compressive ($P_{tip} < 0$) then the axial load has a softening effect typical of beam-column buckling.

IV. Results

Structural deformation and the internal forces and moments were calculated using the least-squares finite element method. The finite element mesh and the deformed joined wing frame are plotted in Fig. 4 (a) and (b), respectively. Figure 5 shows plots of the displacement and the forces in the sting under a static vertical lift load on the tip of the sting. As seen in Fig. 5 (d), (e) and (f), the forces and moments in the sting have a discontinuity at the joint. The element matrix cannot be assembled directly, because the assembly procedure assumes continuity of the state variables. A Multipoint Constraint (MPC) can be used to match the degrees of freedom of the joint nodes. The corresponding displacements and the forces in the strut are plotted in Fig. 6.

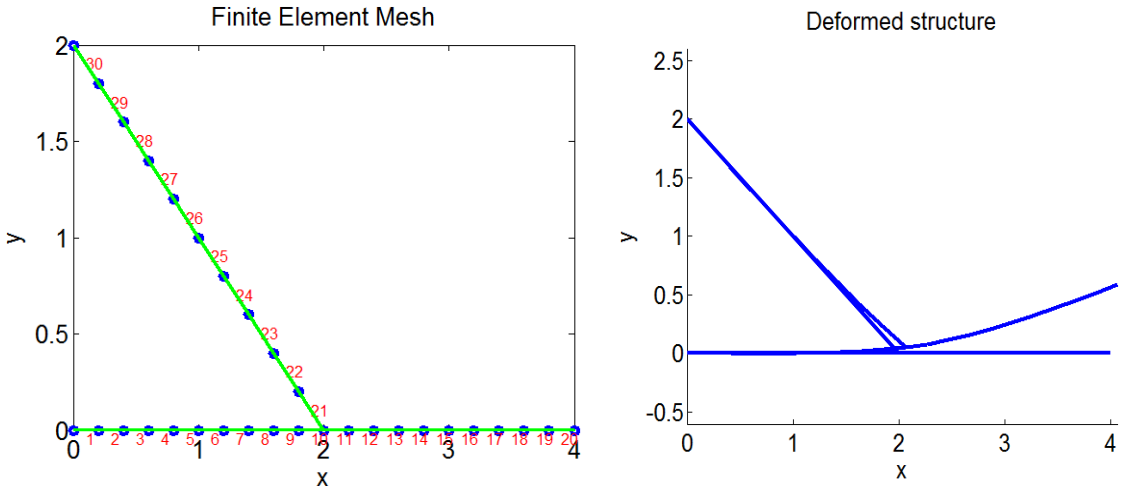

(a) (b)

Figure 4: Finite Element Mesh (a) and the Deformed Joined Wing Structure (b)

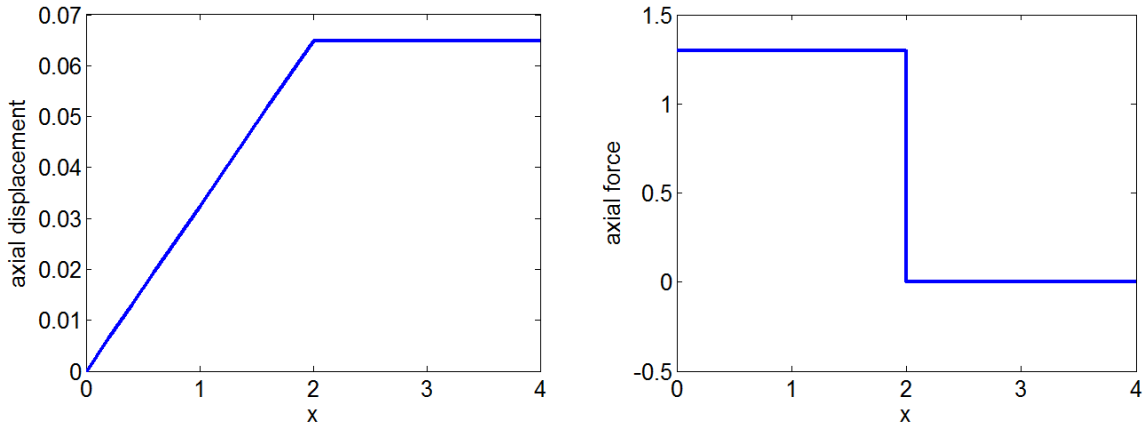

(a) (d)

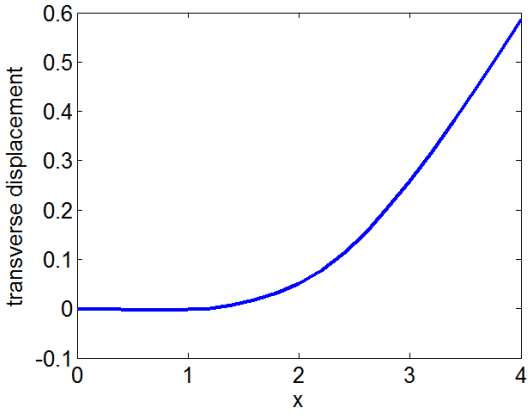

(b)

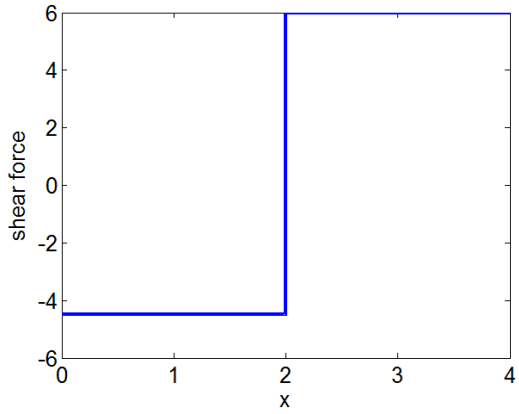

(e)

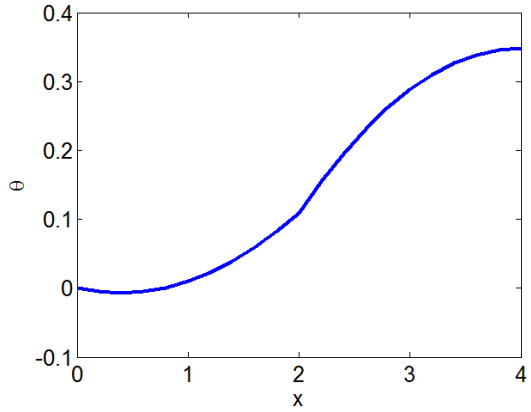

(c)

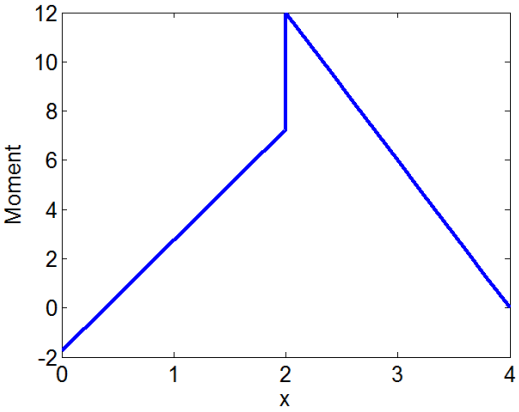

(f)

Figure 5: Displacements (a), (b), (c) and Forces & Moments (d), (e), (f) in Sting

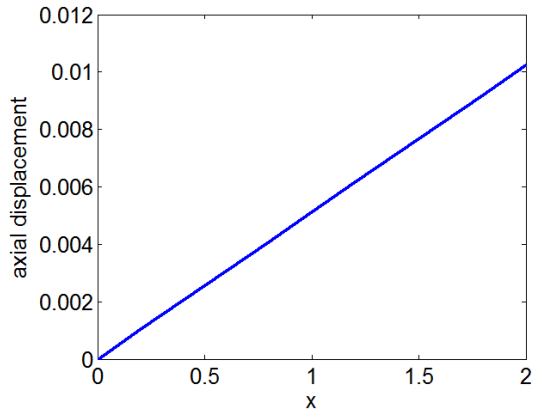

(a)

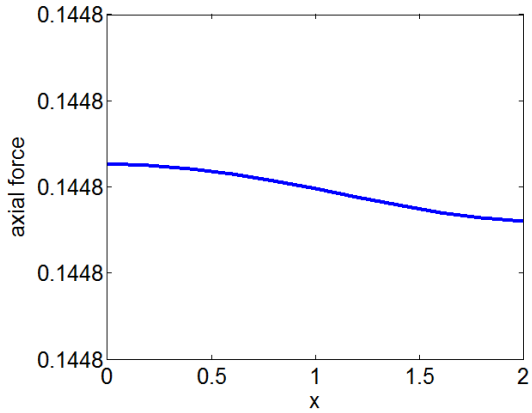

(d)

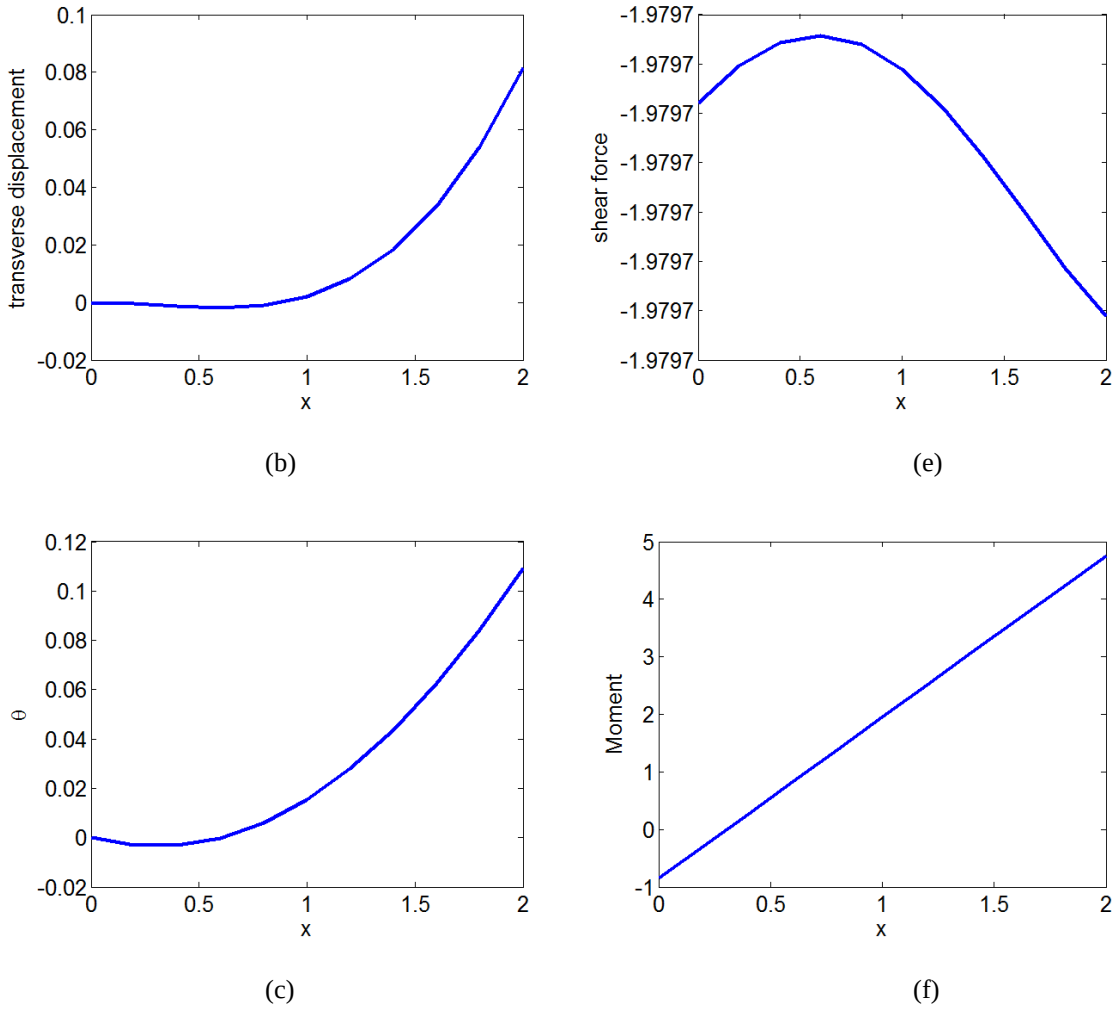

Figure 6: Displacements (a), (b), (c) and Forces & Moments (d), (e), (f) in Strut

Design sensitivity to shape design parameters of the joined beam structure were calculated using the continuous sensitivity equation method. The first shape parameter was the length of the sting and the strut, which changed without a change of reference angles. By definition, the continuous sensitivity variables represent the local derivatives (at the Eulerian point). The CSE total material derivatives are calculated by adding the advection term generated from the original system solution to the local CSE derivatives obtained by solving the CSE equations. The local derivatives were calculated by CSE in this paper and then the total derivatives were calculated by post-processing. Comparison of the local and total CSE sensitivity results with results obtained by finite difference methods are seen in Figs. 7 and 8. Local sensitivity is not equal to the total sensitivity when the convection term is not zero. The finite difference method results, which by nature are the material (total) derivatives, closely match with the total CSE sensitivity results. The second shape sensitivity parameter was the angle β between the strut and the sting. As seen in Fig. 2, $\beta = \beta_a + \beta_f$. For the special case in Fig. 4 (a), $\beta_f = 0$ and $\beta = \beta_a$. CSE results are compared with the finite differences in Figs. 9 and 10.

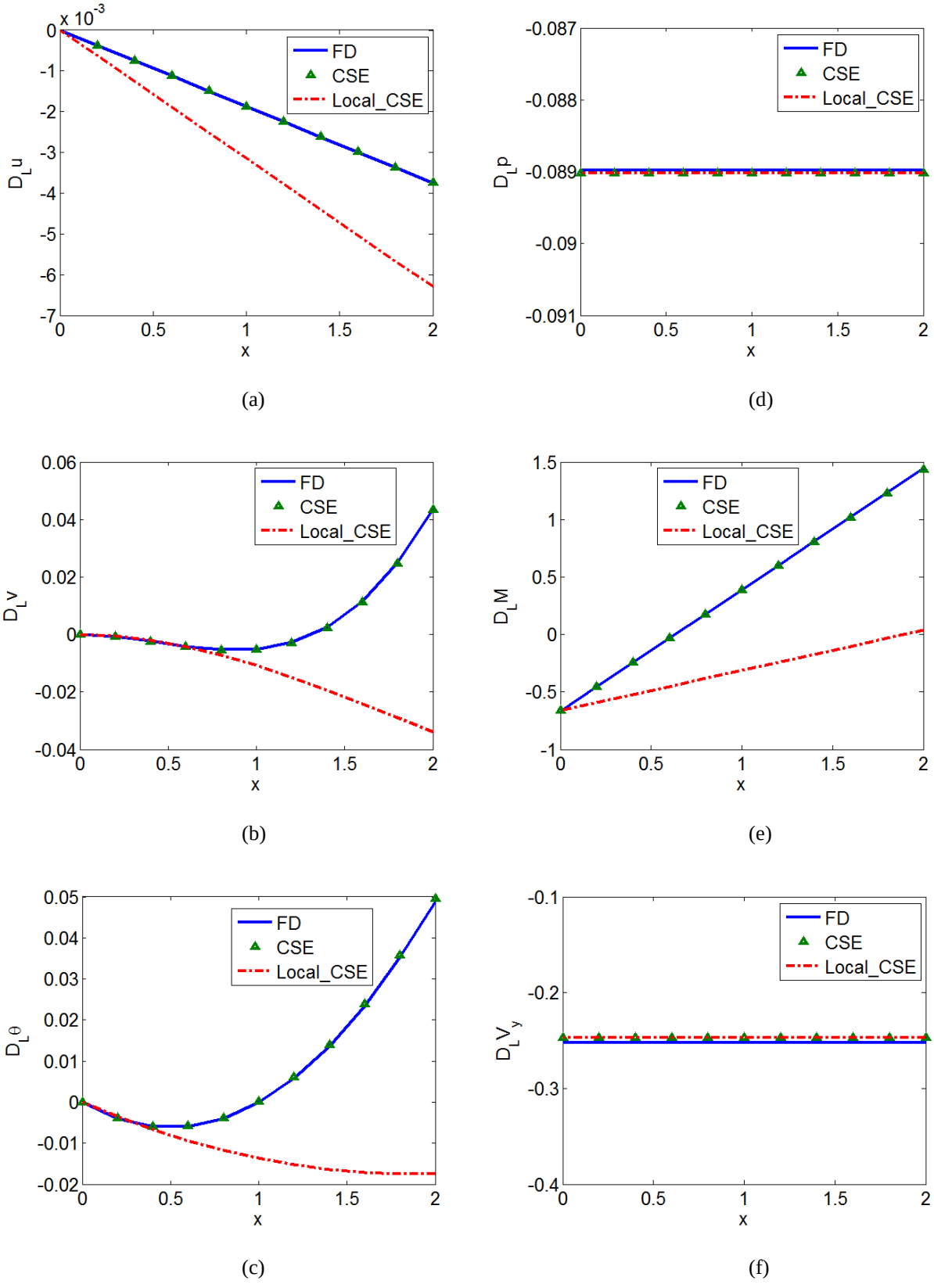

Figure 7: Displacement Sensitivity (a), (b), (c) and Force Sensitivity (d), (e), (f) to L in Strut

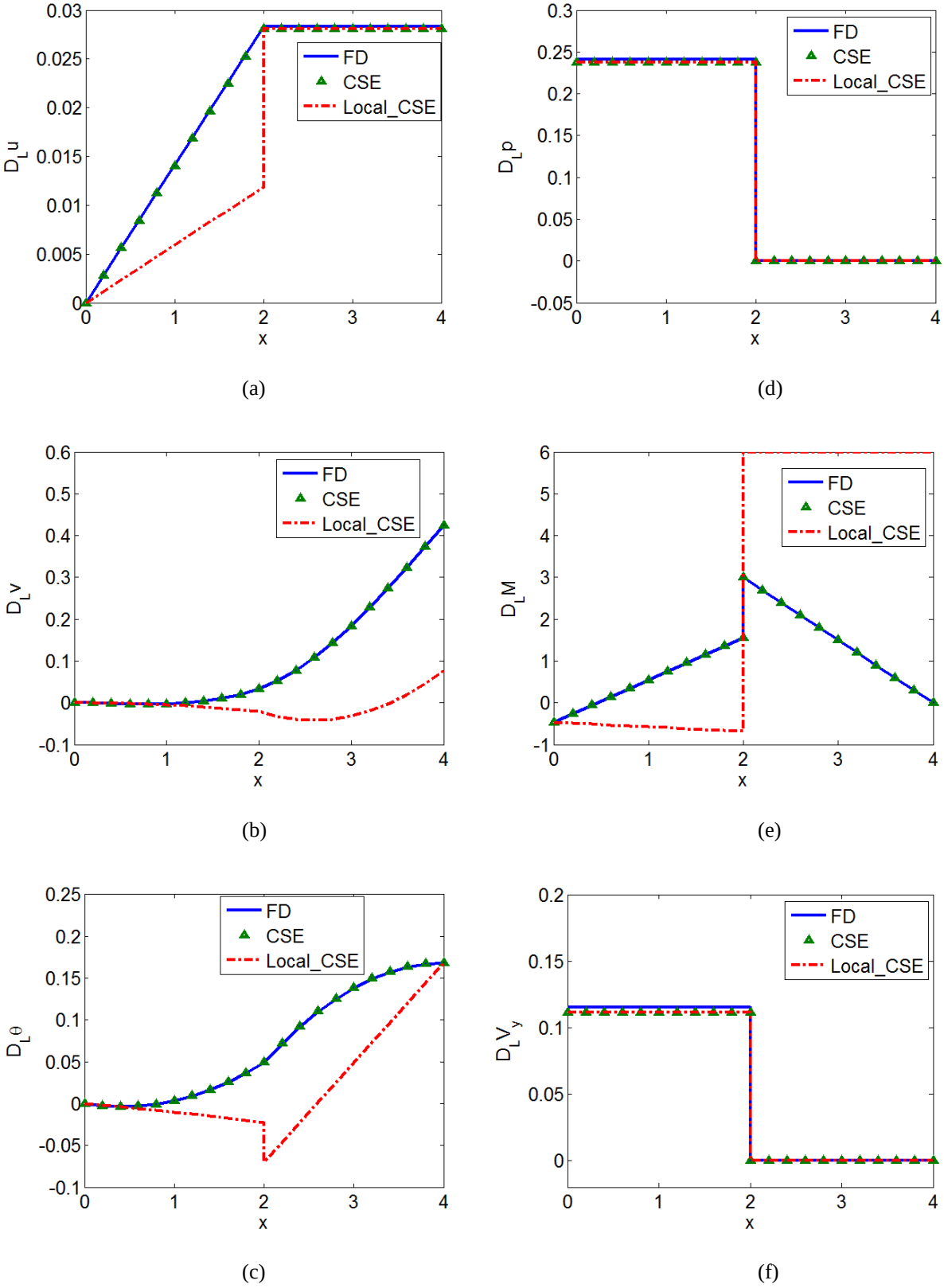

Figure 8: Displacement Sensitivity (a), (b), (c) and Force Sensitivity (d), (e), (f) to L in Sting

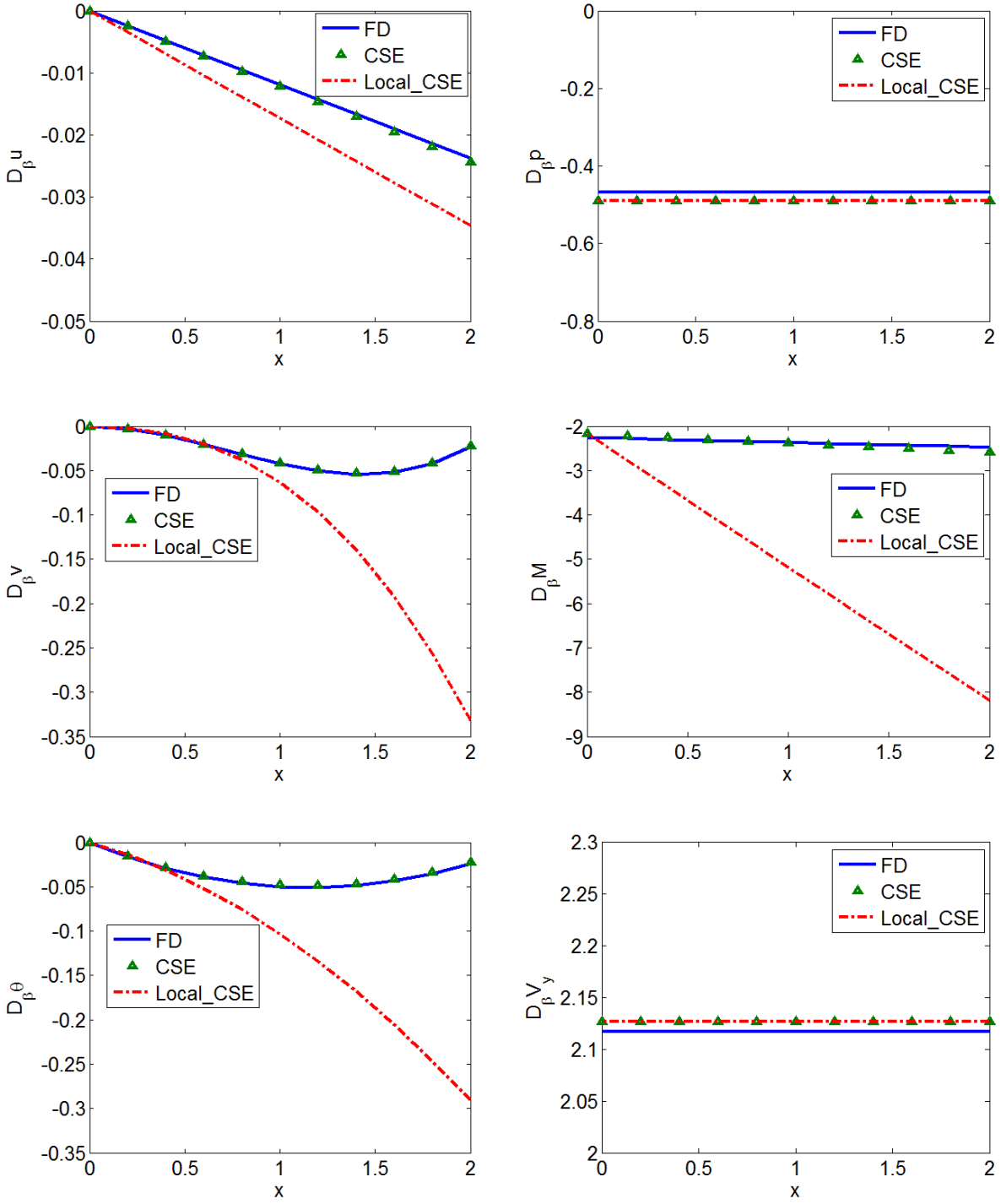

(a) (f)

Figure 9: Displacement Sensitivity (a), (b), (c) and Force Sensitivity (d), (e), (f) to β in Strut

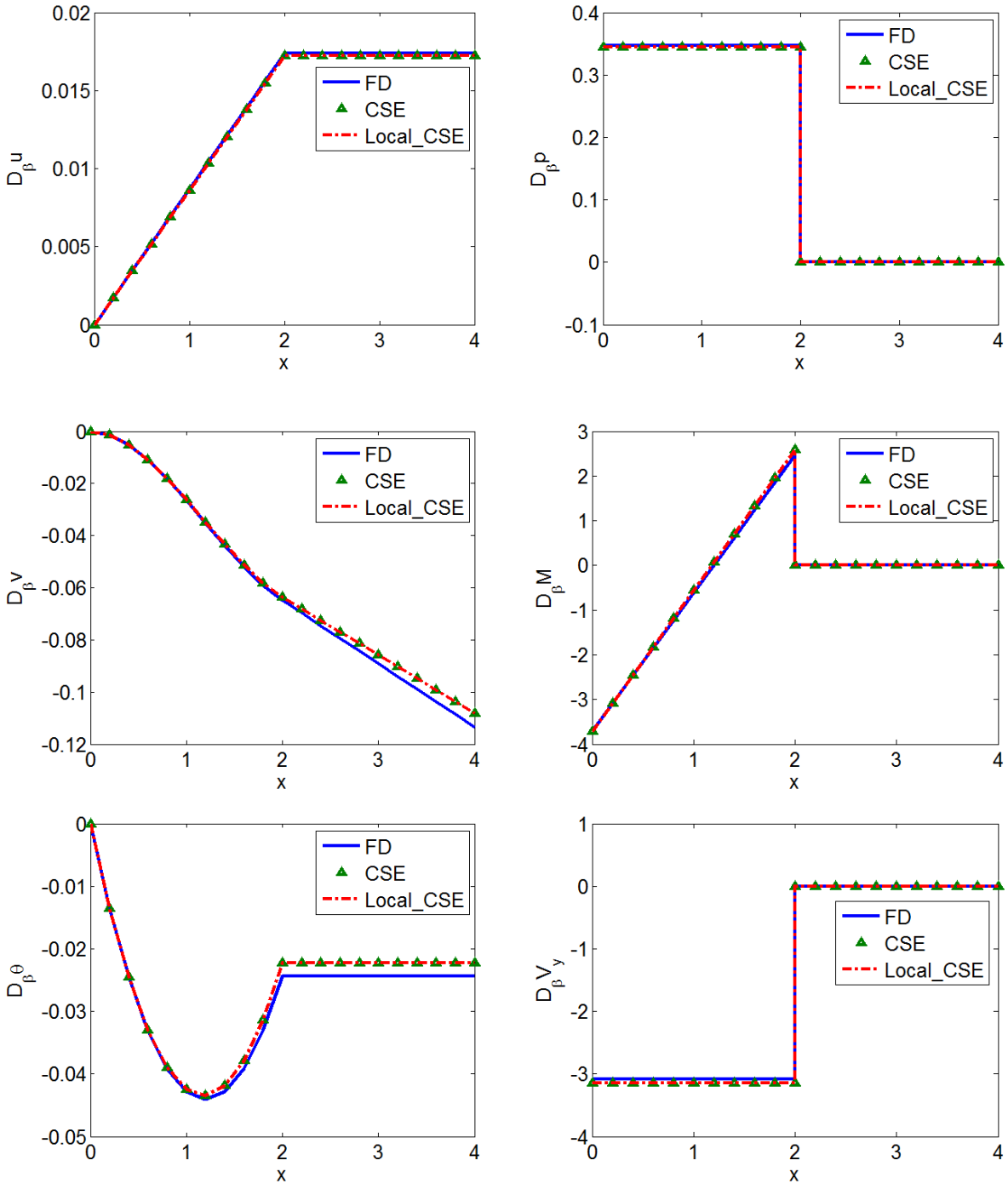

Figure 10: Displacement Sensitivity (a), (b), (c) and Force Sensitivity (d), (e), (f) to β in Sting

Acknowledgements

The Air Force Office of Scientific Research (AFOSR) and the Air Force Research Laboratory (AFRL) Air Vehicles Directorate are funding this research. The authors gratefully acknowledge the support of AFOSR program manager Dr. Fariba Fahroo and the AFRL Senior Aerospace Engineers Dr. Raymond Kolonay, Dr. Phillip Beran, and Dr. Maxwell Blair.

V. References

[1] Rasmussen, C., Canfield, R., and Reddy, J.N., "Nonlinear Transient Gust Response Using a Fully- Coupled Least- Squares Finite Element Formulation," Vol. AIAA-2008-1821, 2008.

[2] Wickert, D.P., Canfield, R.A., and Reddy, J.N., "Fluid-Structure Transient Gust Sensitivity Using Least-Squares Continuous Sensitivity Analysis," 50th AIAA/ASME/ASCE/AHS/ASC Structures, Structural Dynamics, and Materials Conference, Palm Springs, California, May 4-7, 2009, AIAA-2009-2535.

[3] Haug, E.J., Choi, K.K., and Komkov, V., "Design sensitivity analysis of structural systems," *Mathematics in science and engineering*, Vol. 177, Academic Press, Orlando, 1986.

[4] Choi, K.K., and Kim, N.H., "Structural sensitivity analysis and optimization," *Mechanical engineering series*, Springer Science+Business Media, New York, 2005.

[5] Dems, K., and Haftka, R.T., "Two Approaches to Sensitivity Analysis for Shape Variation of Structures," *Mech. Struct. & Mach.*, Vol. 16, No. 4, 1988-1989, pp. 501.

[6] Haftka, R.T., and Gürdal, Z., "Elements of structural optimization," *Solid mechanics and its applications*, Vol. 11, Kluwer Academic Publishers, Dordrecht ; Boston, 1992.

[7] Borggaard, J., and Burns, J., "A PDE Sensitivity Equation Method for Optimal Aerodynamic Design," *Journal of Computational Physics*, Vol. 136, 1997, pp. 366--384.

[8] Dems, K., and Mroz, Z., "Variational approach to first- and second-order sensitivity analysis of elastic structures," *International Journal for Numerical Methods in Engineering*, Vol. 21, 1985, pp. 637-661.

[9] Borggaard, J., and Burns, J., "A Sensitivity Equation Approach to Shape Optimization in Fluid Flows," Langley Research Center, NASA Contractor Report 191598 (ICASE Report No. 94-8), 1994.

[10] Bhaskaran, R., and Berkooz, G., "Optimization of Fluid-Structure Interaction using the Sensitivity Equation Approach," *Fluid-Structure Interaction, Aeroelasticity, Flow-Induced Vibrations and Noise*, Vol. 1, No. 53-1, 1997, pp. 49-56.

[11] Turgeon, E., Pelletier, D., and Borggaard, J., "A Continuous Sensitivity Equation Approach to Optimal Design in Mixed Convection," Vol. AIAA 99-3625, 1999.

[12] Stanley, L.G.D., and Stewart, D.L., "Design sensitivity analysis : computational issues of sensitivity equation methods," *Frontiers in applied mathematics*, Society for Industrial and Applied Mathematics, Philadelphia, 2002, pp. 139.

[13] Wickert, D.P., Roberts, R.W., and Canfield, R.A., "Least-Squares Continuous Sensitivity Equations for an Infinite Plate with a Hole," Vol. AIAA-2008-1797, 2008.

[14] Étienne, S., and Pelletier, D., "A general approach to sensitivity analysis of fluid–structure interactions," *Journal of Fluids and Structures*, Vol. 21, No. 2, 2005, pp. 169-186.

[15] Etienne, S., Hay, A., Garon, A., "Shape Sensitivity Analysis of Fluid-Structure Interaction Problems," Vol. AIAA 2006-3217, AIAA, 2006.

[16] Etienne, S., Hay, A., Garon, A., "Sensitivity Analysis of Unsteady Fluid-Structure Interaction Problems," Vol. AIAA-2007-332, AIAA, 2007.

[17] Dems, K., and Mroz, Z., "Variational approach by means of adjoint systems to structural optimization and sensitivity analysis. I - Variation of material parameters within fixed domain," *International Journal of Solids and Structures*, Vol. 19, No. 8, 1983, pp. 677-692.

[18] Livne, E., "Future of Airplane Aeroelasticity," *Journal of Aircraft*, Vol. 40, No. 6, 2003, pp. 1066--1092.

[19] Bendiksen, O.O., "Modern developments in computational aeroelasticity," *Journal of Aerospace Engineering*, Vol. 218, 2004, pp. 157.

[20] Hubner, B., Walhorn, E., and Dinkler, D., "A monolithic approach to fluid–structure interaction using space–time finite elements," *Computer Methods in Applied Mechanics and Engineering*, 2004.

[21] Etienne,S. (Ecole Polytechnique de Montreal), "A monolithic formulation for unsteady Fluid-structure Interactions," *Collection of Technical Papers - 44th AIAA Aerospace Sciences Meeting, Collection of Technical Papers - 44th AIAA Aerospace Sciences Meeting*, Vol. 11, 2006, pp. 8301.

[22] Walhorn, E., Kölke, A., Hübner, B., "*Fluid-structure coupling within a monolithic model involving free surface flows*," *Computers and Structures*, Vol. 83, 2005, pp. 2100-2111.

[23] Heys, J.J., Manteuffel, T.A., McCormick, S.F., "First-order system least squares (FOSLS) for coupled fluid-elastic problems," *Journal of Computational Physics*, Vol. 195, No. 2, 2004, pp. 560-575.

[24] Bathe, K., and Zhang, h., "Finite element developments for general fluid flows with structural interactions," *International Journal for Numerical Methods in Engineering*, Vol. 60, 2004, pp. 213-213-232.

[25] Bathe, K., and Shanhong, H.Z., "Finite element analysis of fluid flows fully coupled with structural interactions," *Computer and Structures*, Vol. 72, 1999, pp. 1-1-16.
[26] Kayser-Herold, O., and Matthies, H.G., "A Unified Least-Squares Formulation for Fluid-Structure Interaction Problems," *Computer and Structures*, Vol. 85, 2007, pp. 998-998-1011.
[27] Rasmussen, C.C., Canfield, R.A., and Reddy, J.N., "The Least-Squares Finite Element Method Applied to Fluid-Structure Interaction Problems," AIAA, 2007.
[28] Bochev, P.B., and Gunzburger, M.D., "Finite Element Methods of Least-Squares Type," *SIAM Review*, Vol. 40, No. 4, 1998, pp. 789--837.
[29] Jiang, B., "The least-squares finite element method : theory and applications in computational fluid dynamics and electromagnetics," *Scientific computation*, Springer, Berlin ; New York, 1998, pp. 418.
[30] Yang, S., and Liu, J., "Analysis of Least Squares Finite Element Methods for A Parameter-Dependent First-Order System," *Numerical Functional Analysis and Optimization*, Vol. 19, 1998, pp. 191-213.
[31] Bramble, J.H., Lazarov, R.D., and Pasciak, J.E., " Least-squares methods for linear elasticity based on a discrete minus one inner product." *Comput. Methods Appl. Mech. Engrg.*, Vol. 152, 2001, pp. 520--543.
[32] Proot, M.M.J., "The least-squares spectral element method: theory, implementation and application to incompressible flows," 2003.
[33] Cai, Z., Manteuffel, T., McCormick, S., " *First-order system least squares for the Stokes equations, with application to linear elasticity*," *SIAM Journal of Numerical Analysis*, Vol. 34, No. 5, 1997, pp. 1727--1741.
[34] Pontaza, J.P., "Least-squares finite element formulation for shear-deformable shells," *Computer Methods in Applied Mechanics and Engineering*, Vol. 194, No. 21-24, 2005, pp. 2464.
[35] Kayser-Herold, O., and Matthies, H.G., "Least-Squares FEM Literature Review," Institute of Scientific Computing Technical University Braunschweig, 2005-05, Brunswick, Germany, 2005.
[36] Blair, M., Canfield, R.A., and Roberts, R., "A Joined-Wing Aeroelastic Design with Geometric Non-Linearity," *Journal of Aircraft*, Vol. 42, No. 4, 2005, pp. 832-832–848.
[37] Demasi, L., and Livne, E., "Exploratory Studies of Joined Wing Aeroelasticity," AIAA, 2005.
[38] Hoblit, F.M., "Gust loads on aircraft : concepts and applications," *AIAA education series*, American Institute of Aeronautics and Astronautics, Washington, D.C., 1988, pp. 306.
[39] Reddy, J.N., "An introduction to nonlinear finite element analysis," Oxford University Press, Oxford ; New York, 2004, pp. 463.
[40] Gel'fand, I.M., Fomin, S.V., and Silverman, R.A., "Calculus of variations," Dover Publications, Mineola, N.Y., 2000.
[41] Reddy, J.N., "An introduction to the finite element method," *McGraw-Hill series in mechanical engineering*, McGraw-Hill Higher Education, New York, NY, 2006.
[42] Šolin, P., Segeth, K., and Doležel, I., "Higher-order finite element methods," *Studies in advanced mathematics*, Chapman & Hall/CRC, Boca Raton, FL, 2004.
[43] Szabo, B.A., and Babuška, I., "Finite element analysis," Wiley, New York, 1991.